Available online at www.sciencedirect.com
SCIENCE DIRECT®
Journal of Solid State Chemistry 172 (2003) 95–101
JOURNAL OF SOLID STATE CHEMISTRY
http://elsevier.com/locate/jssc

The crystal structure of synthetic simmonsite, Na_2LiAlF_6

Kirk C. Ross,[a] Roger H. Mitchell,[a,*] and Anton R. Chakhmouradian[b]

[a] Department of Geology, Lakehead University, 955 Oliver Road, Thunder Bay, Ont., Canada P7B 5E1
[b] Department of Geological Sciences, University of Manitoba, Winnipeg, Man., Canada R3T 2N2

Received 5 August 2002; received in revised form 17 October 2002; accepted 29 October 2002

Abstract

The structure of the synthetic fluoroperovskite, Na_2LiAlF_6 (simmonsite), has been determined by powder X-ray diffraction using the Rietveld method of structure refinement. The compound adopts space group $P2_1/n$ [#14; $a = 5.2842(1)$; $b = 5.3698(1)$; $c = 7.5063(2)$ Å; $\beta = 89.98(1)^\circ$; $Z = 4$), and is a member of the cryolite (Na_2NaAlF_6) structural group characterized by ordering of the *B*-site cations (Li, Al) and tilting of the BF_6 octahedra according to the tilt scheme $a^-b^-c^+$. Rotations of the *B*-site polyhedra are less ($\Phi_{Li} = 14.9^\circ$; $\Phi_{Al} = 17.0^\circ$) than those found in cryolite ($\Phi_{Na} = 18.6$; $\Phi_{Al} = 23.5^\circ$) because of the larger difference in the ionic radii of the *B*-site cations in cryolite as compared to those in simmonsite. Na at the *A*-site is displaced from the special position resulting in 10- and 8-fold coordination in simmonsite and cryolite, respectively. By analogy with the synthetic compound, naturally occurring simmonsite is considered to adopt space group $P2_1/n$ (#14) and not the $P2_1$(#4) or $P2_1/m$(#11) space groups.

Keywords: Perovskite; Cryolite; Simmonsite; Rietveld refinement

1. Introduction

With the exception of perovskite-structured $MgSiO_3$ which is considered to constitute the majority of the lower mantle of the Earth, naturally occurring oxide minerals with the perovskite ABX_3 structure are principally titanates and niobates [1]. Until the recent discovery of simmonsite (Na_2LiAlF_6) by Foord et al. [2], naturally occurring fluoro-perovskites were represented only by the minerals elpasolite (K_2NaAlF_6), cryolite (Na_2NaAlF_6) and neighborite ($NaMgF_3$) [3]. In contrast, numerous fluorides which adopt the perovskite structure have been synthesized [4]. Many of these form simple ternary compounds with the stoichiometry ABF_3, where *A* and *B* are monovalent and divalent cations, respectively. Others are complex or double perovskites $A_2BB'F_6$ (A = Na, K, Rb, NH_4; B = Li, Na; B' = Al, Sc, Fe, Ga) belonging principally to the elpasolite [space group $Fm\bar{3}m$ (#225) or cryolite [space group $P2_1/n$(#14)] structural groups [3]. The structure of natural simmonsite was not determined in the original description as the specimen investigated was complexly twinned, although it was recognized that the mineral is not cubic and has monoclinic symmetry. On the basis of previous studies (see below) of the structure of synthetic Na_2LiAlF_6 [5–6] it was suggested by Foord et al. [2] that the compound adopts either the $P2_1$ (#4) or $P2_1/m$(#11) space groups.

Garton and Wanklyn [5] investigated the system Na_3AlF_6–Li_3AlF_6 by differential thermal analysis and powder X-ray diffraction, and claimed that below 500°C a compound corresponding in composition to Na_2LiAlF_6 was hexagonal ($a = 5.30(0)$ Å; $c = 13.09(5)$ Å), regardless of the presence of several weak reflections in violation of hexagonal symmetry. Subsequently, Holm and Holm [6] re-investigated the same system and described Na_2LiAlF_6 as a **B**-face centered monoclinic compound with lattice parameters: $a = 7.538$ Å; $b = 7.516$ Å; $c = 7.525$Å; $\beta = 90.81^\circ$, $Z = 4$; at 20°C. Foord et al. [2] have conducted single crystal and powder X-ray diffraction work on the natural material and recognized that it has a perovskite structure. Following the older literature [7] in which $CaTiO_3$ orthorhombic perovskite is described in terms of a monoclinic cell they suggested that simmonsite is isostructural with a "monoclinic" double perovskite, $Ca_2Ti_2O_6$, and indexed the powder XRD pattern on a

*Corresponding author. Fax: +807-346-7853.
E-mail address: rmitchel@gale.lakeheadu.ca (R.H. Mitchell).

0022-4596/03/$ - see front matter © 2003 Elsevier Science (USA). All rights reserved.
doi:10.1016/S0022-4596(02)00137-8

doubled ($\approx 2a_p$) unit cell [$a = 7.5006(6)$; $b = 7.474(1)$; $c = 7.503(1)$ Å; $\beta = 90.487^\circ(9)$] in space group $P2_1/m$(#11). Foord et al. [2] were unable to determine the structure of natural simmonsite by single crystal methods as the mineral is complexly twinned. However, they indicate that it has similar cell dimensions and β angle to $CaTiO_3$ and suggest that the apparent $h0l$ *n*-glide present in their XRD data is an artifact of pseudo-**B**-centering. Foord et al. [2] mention the presence of several weak reflections in violation of monoclinic symmetry but do not list these.

Assuming that the *B*-site cations are completely ordered none of the above proposed space groups are maximal sub-groups of the aristotype $Fm\bar{3}m$ (#225) elpasolite structure [8]. Anderson et al. [9] and Woodward [10] have discussed ordering in $A_2BB'X_6$ double perovskites and noted that the following space groups are possible: (1) *Pbnm* (#62), no ordering plus octahedron tilting; (2) $Fm\bar{3}m$ (#225), rock salt ordering and no tilting of octahedra; (3) $P2_1/n$ (#14), rock salt ordering plus octahedron tilting; (4) $P2_1/m$ (#11), layered structures with octahedron tilting. Each space group is characterized by powder XRD patterns which exhibit characteristic peak splittings, superlattice reflections and systematic absences (see below).

Ordering can be expected in Na_2LiAlF_6 because of the charge difference between Li^+ and Al^{3+}. Differences in *B*-site cation ionic radii are not as significant for Na_2LiAlF_6 (0.21 Å) as for Na_2NaAlF_6 (0.79 Å), and the former compound should have a lesser propensity to order than the latter on the basis of this criterion alone. Of the 1:1 ordered perovskites those which crystallize in space group $P2_1/m$ (#11) are extremely rare; the only example known being La_2CuSnO_6, in which layers of CuO_6 and SnO_6 alternate along [001]. Anderson and Poeppelmeier [11] suggest that the presence of an ion which shows the Jahn–Teller effect is required to stabilize the layering, hence it is unlikely that Na_2LiAlF_6 will adopt this space group.

From inspection of the powder XRD pattern of Na_2LiAlF_6 (Fig. 1) it is evident that the compound does not possess $Fm\bar{3}m$ (#225) symmetry as superlattice reflections and split peaks are present. As the Goldschmidt tolerance factor (t) of 1:1 ordered Na_2LiAlF_6 is 0.949 it is proposed that reduction in symmetry from $Fm\bar{3}m$ (#225) must take place by rotation of the LiF_6

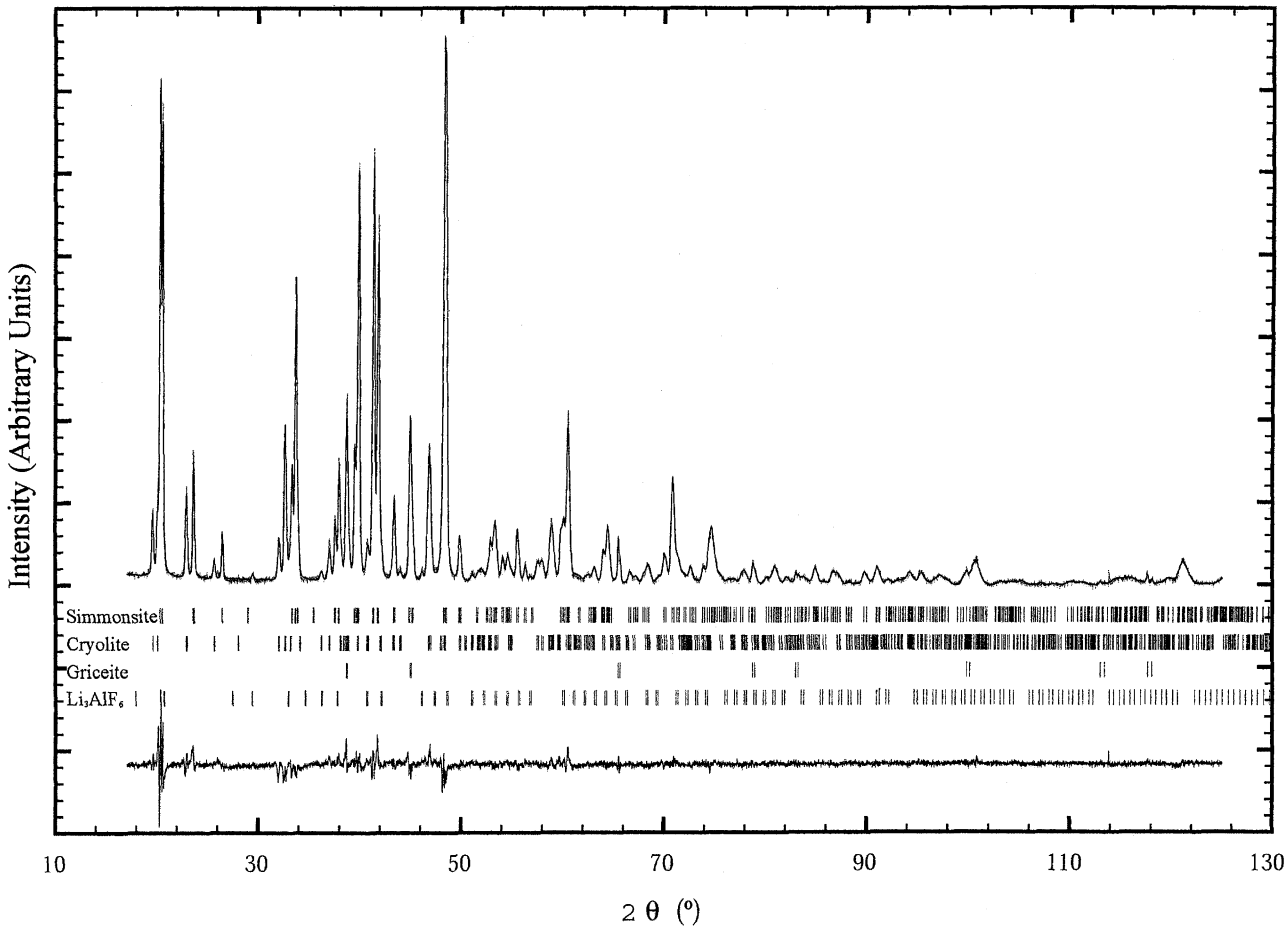

Fig. 1. Rietveld difference plot of synthetic simmonsite.

and AlF_6 polyhedra in a manner similar to that found for the cryolite structure ($t = 0.876$) resulting in the derivative or hettotype $P2_1/n$ (#14) space group [9,10]. Consequently, we suggest that previous studies have failed to consider adequately the origin of the superlattice reflections present in the powder XRD patterns of synthetic and natural simmonsite. In order to resolve the existing ambiguities we have re-investigated the structure of synthetic simmonsite by Rietveld methods.

2. Experimental

Simmonsite and cryolite were synthesized from stoichiometric mixtures of pre-dried NaF (99.99%), LiF (99.99%) and AlF_3 (99.99%) (all Aldrich Chemical Co.). The starting reagents were mixed in an agate mortar under acetone and heated in an evacuated quartz tube followed by rapid quenching in air. With respect to Na_2LiAlF_6 we tried several synthesis temperatures and times but were unable to synthesize material free of contaminant phases, and minor amounts (total <10 wt%) of $P2_1/n$ (#14) Na_2NaAlF_6 (cryolite), $Fm\bar{3}m$ (#225) LiF (griceite) and $Pna2_1$ (#33) Li_3AlF_6 were present in all preparations. Synthesis at 650°C for 24 h produced run products with the least amounts of contaminating phases.

Powder X-ray diffraction (XRD) data were collected using a Phillips P3710 diffractometer with APD powder diffraction software. XRD step scans were collected using a 0.02° step for 4 s over a range of 10–125° 2θ with monochromatic Cu$K\alpha$ radiation. The XRD patterns were initially inspected visually and further analyzed by CELREF [12] and/or the Rietveld method using the FULLPROF (FP2K) program [13]. The 10–17° 2θ range was initially excluded from the Rietveld profile analysis as this region contained no reflections and problems were experienced in defining the background fitting function. However, this region was included in the final stage of the profile fitting which incorporated instrumental, structural and thermal parameters together with a pseudo-Voigt peak shape function. Site occupancies were not refined and *B*-site ordering was considered to be ideal. Attempts to refine *B*-site occupancies resulted in instability and no convergence of the refinement and/or significantly increased agreement parameters. All refinements included the three possible contaminant phases. Structural data for these phases are not incorporated into this work as the small amounts present resulted in poor Rietveld agreement parameters.

3. Space group assignment

Analysis of the XRD patterns by inspection and CELREF indicated that the most probable space group of synthetic Na_2LiAlF_6 is $P2_1/n$ (#14). This conclusion is based upon the presence of split reflections which rule out $Pm\bar{3}m$ (#221) and $Fm\bar{3}m$ (#225) space groups. Distinction between $P2_1/n$ (#14) and $Pbnm$ (#62) is based upon systematic absences. In $Pbnm$ (#62) reflections of the type: $h\,0\,l$ ($h+l=2n+1$); $0kl$ ($k=2n+1$); $h\,0\,0$ ($h=2n+1$); $0\,k\,0$ ($k=2n+1$); and $0\,0\,l$ ($l=2n+1$) are absent. In $P2_1/n$ (#14) the systematic absences are the same except the $0kl$ ($k=2n+1$) condition is lifted [9]. Hence the presence of $0kl$ ($k=2n+1$) reflections, e.g., 0 1 1, 0 3 1, is evidence that the ordering of the *B*-site cations is present. Monoclinic symmetry is indicated by the splitting of cubic lattice peaks indexed on a doubled perovskite cell ($2a_p$) into monoclinic doublets i.e., 400_{2ap} into the $P2_1/n$ 2 2 0 and 0 0 4 peaks [3,10]. Table 1 lists diffraction lines for synthetic Na_2LiAlF_6 indexed in the space group $P2_1/n$ (#14). Note the presence of reflections indicating rock salt ordering i.e., 0 1 1, 1 0 1 and monoclinic symmetry e.g., 2 2 0 and 0 0 4. The compounds cannot be satisfactorily indexed using the doubled perovskite cell as required by $P2_1/m$ (#11) symmetry. Indexing the powder XRD pattern of natural simmonsite (from 20–50° 2θ) using CELREF and data given by Foord

Table 1
Calculated and observed 2θ (20–50°), *d*-spacings and indices for synthetic $P2_1/n$ simmonsite Na_2LiAlF_6

h	k	l	d(Å)$_{calc}$	$2\theta_{calc}$	I_{calc}	d(Å)$_{obs}$	$2\theta_{obs}$	I_{obs}
0	1	1	4.3674	20.33	67	4.36742	20.32	65
1	0	1	4.3219	20.55	24	4.32187	20.53	24
1	0	−1	4.3202	20.56	37	4.32019	20.54	36
1	1	0	3.7665	23.62	13	3.76648	23.60	15
0	0	−2	3.7532	23.71	6	3.75323	23.69	7
1	1	1	3.3669	26.47	3	3.36686	26.45	3
1	1	−1	3.3661	26.48	4	3.36606	26.46	3
0	2	0	2.6849	33.37	17	2.68495	33.34	16
1	1	2	2.6590	33.71	27	2.65900	33.68	26
1	1	−2	2.6582	33.72	24	2.65822	33.69	23
2	0	0	2.6422	33.93	10	2.64217	33.90	9
1	2	0	2.3937	37.57	11	2.39369	37.54	11
2	1	0	2.3707	37.95	18	2.37074	37.92	19
1	2	1	2.2807	39.51	21	2.28067	39.48	21
1	2	−1	2.2804	39.52	1	2.28042	39.48	1
0	1	−3	2.2680	39.74	2	2.26802	39.71	2
1	0	3	2.2618	39.85	11	2.26181	39.82	11
1	0	−3	2.2611	39.87	26	2.26109	39.84	28
2	1	1	2.2609	39.87	27	2.26091	39.84	28
2	1	−1	2.2604	39.88	5	2.26043	39.85	5
0	2	−2	2.1837	41.34	81	2.18371	41.31	83
2	0	2	2.1609	41.80	31	2.1609	41.77	34
2	0	−2	2.1601	41.82	32	2.16009	41.78	35
1	1	3	2.0845	43.41	5	2.08445	43.48	5
1	1	−3	2.0839	43.42	7	2.08389	43.39	7
1	2	2	2.0184	44.91	10	2.01835	44.87	11
1	2	−2	2.0180	44.92	8	2.01801	44.88	9
2	1	2	2.0047	45.23	5	2.00470	45.19	6
2	1	−2	2.0040	45.25	5	2.00403	45.21	6
2	2	0	1.8832	48.33	100	1.88324	48.29	100
0	0	−4	1.8766	48.51	54	1.87620	48.47	57

et al. [2] also indicates that mineral adopts $P2_1/n$ symmetry (#14; $a = 5.242$ Å, $b = 5.259$ Å, $c = 7.644$ Å, $\beta = 91.848$). Indexing in this space group ($msd = 0.058$) gives a better fit to these data than $P2_1/m$ (#11; $msd = 0.124$), and satisfactorily indexes many of the weaker higher angle lines.

The monoclinic 0 1 1 reflection indicating rock salt ordering is less intense in synthetic Na_2LiAlF_6 (Table 1) than in the natural material, for which 0 1 1 is the strongest diffraction line [2]. This suggests that the synthetic material is actually only partially ordered. We attempted to refine the site occupancies of Li and Na but found the refinement to be unstable with no convergence. Resolution of this question by a neutron diffraction study is planned but is not central to the purpose of this paper which is to determine the space group of Na_2LiAlF_6.

4. Rietveld refinement

We were initially uncertain if alumino-fluoroperovskite structures could be adequately characterized and refined by Rietveld profile analysis using conventional laboratory XRD techniques. Therefore, as a test of the profile analysis method we X-rayed natural cryolite from Ivigtut (Greenland) and refined the structure with FULLPROF using the data of Hawthorne and Ferguson [14] as starting crystallographic parameters for the model (Table 1). Our data are in excellent agreement with those of Hawthorne and Ferguson [14] with respect to atomic coordinates of the ions, cell dimensions and bond lengths (Table 2). Secondly, synthetic cryolite was structurally refined by the same methods. Table 3 lists the final agreement and crystallographic parameters for synthetic cryolite. These data demonstrate clearly that alumino-fluoroperovskites are amenable to Rietveld structural analysis using laboratory X-ray diffraction data.

The XRD data for synthetic simmonsite were initially refined in three different space groups: $P2_1$ (#4); $P2_1/m$ (#11); and $P2_1/n$ (#14). Final output files for the first two space groups yielded unacceptable agreement parameters, i.e., $R_{Bragg} = 34.8\%$ and $R_{Bragg} = 14.62\%$, together with spurious values for thermal isotropic vibrations. The poor agreement parameters were attributed to the presence of intense $h\,0\,l$ reflections in the observed pattern where $(h + l = 2n)$, i.e., 202 at 41.8° 2θ. Refinement in the space group $P2_1/n$ (#14) accounted for these reflections and gave the best agreement ($R_{Bragg} = 3.15\%$) and thermal parameters. Fig. 1 is a Rietveld difference plot of the observed and calculated patterns for synthetic Na_2LiAlF_6 (simmonsite) in space group $P2_1/n$ (#14), with crystallographic parameters being given in Table 3.

Table 2
Positional and thermal parameters for natural cryolite, Na_2NaAlF_6 in space group $P2_1/n$

		x	y	z	B
Natural cryolite (this work)					
Al	*2a*	0	0	0	0.9(1)
Na(1)	*2b*	0	0	0.5	1.4(1)
Na(2)	*4e*	0.5119(5)	0.9489(1)	0.2488(7)	2.4(1)
F(1)	*4e*	0.1036(6)	0.0442(6)	0.2196(7)	1.3(2)
F(2)	*4e*	0.7257(7)	0.1741(1)	0.0425(1)	1.9(2)
F(3)	*4e*	0.1693(7)	0.2683(7)	−0.0609(6)	1.8(2)
Natural cryolite (Hawthorne & Ferguson [14])					
Al	*2a*	0	0	0	0.67(2)
Na(1)	*2b*	0	0	0.5	1.07(2)
Na(2)	*4e*	0.5133(2)	0.9481(2)	0.2474(1)	1.55(2)
F(1)	*4e*	0.1062(2)	0.0455(2)	0.2194(2)	1.31(2)
F(2)	*4e*	0.7268(2)	0.1737(2)	0.0462(2)	1.34(2)
F(3)	*4e*	0.1634(2)	0.2609(2)	−0.0630(2)	1.39(2)

Natural cryolite (this work; powder XRD—Rietveld method): $a = 5.4058(2)$, $b = 5.5926(2)$, $c = 7.7699(3)$Å, $\beta = 90.195(1)°$; $R_p = 12.9\%$; $R_{wp} = 15.3\%$; $R_{exp} = 8.05\%$; $R_{Bragg} = 6.41\%$; $\chi^2 = 3.6$. Mean bond lengths: Al–F = 1.812; Na(1) = 2.246; Na(2) = 2.502.
Natural cryolite (Hawthorne & Ferguson [14]); single crystal XRD: $a = 5.4024(2)$, $b = 5.5959(2)$, $c = 7.7564(3)$Å, $\beta = 90.28(1)°$; $R_{Bragg} = 3.3\%$. Mean bond lengths: Al–F = 1.8016; Na(1)–F = 2.256; Na(2)–F = 2.499Å.

Table 3
Positional and thermal parameters for synthetic Na_2LiAlF_6 (simmonsite) and Na_2NaAlF_6 (cryolite)

		x	y	z	B
Na_2LiAlF_6 (simmonsite)					
Li	*2c*	0.5	0	0.5	1.0(1)
Al	*2d*	0.5	0	0	1.4(1)
Na	*4e*	0.5010(6)	0.5389(3)	0.2506(5)	2.1(1)
F(1)	*4e*	0.2200(6)	0.1930(6)	0.9620(8)	1.4(2)
F(2)	*4e*	0.3072(6)	0.7215(6)	0.9585(7)	1.5(2)
F(3)	*4e*	0.4239(5)	0.9796(4)	0.2310(8)	1.4(2)
Na_2NaAlF_6 (cryolite)					
Na(1)	*2c*	0.5	0	0.5	1.6(1)
Al	*2d*	0.5	0	0	1.8(1)
Na(2)	*4e*	0.5138(5)	0.5520(4)	0.2518(5)	2.3(1)
F(1)	*4e*	0.2255(7)	0.1765(7)	0.9530(6)	1.6(1)
F(2)	*4e*	0.3353(7)	0.7285(7)	0.9362(6)	1.4(1)
F(3)	*4e*	0.3970(6)	0.9564(6)	0.2182(6)	1.4(1)

Simmonsite: $a = 5.2842(1)$, $b = 5.3698(1)$, $c = 7.5063(2)$Å, $\beta = 89.98(1)°$; $Z = 4$; $R_p = 9.19\%$; $R_{wp} = 11.5\%$; $R_{exp} = 7.07\%$; $R_{Bragg} = 3.15\%$; $\chi^2 = 2.63$. Cryolite: $a = 5.054(1)$, $b = 5.5934(1)$, $c = 7.7672(1)$Å, $\beta = 89.81(1)°$; $R_p = 14.30\%$; $R_{wp} = 16.80\%$; $R_{exp} = 8.73\%$; $R_{Bragg} = 5.93\%$; $\chi^2 = 3.71$.

5. Discussion

We consider that synthetic simmonsite, in common with cryolite, adopts space group $P2_1/n$ (#14) and is a

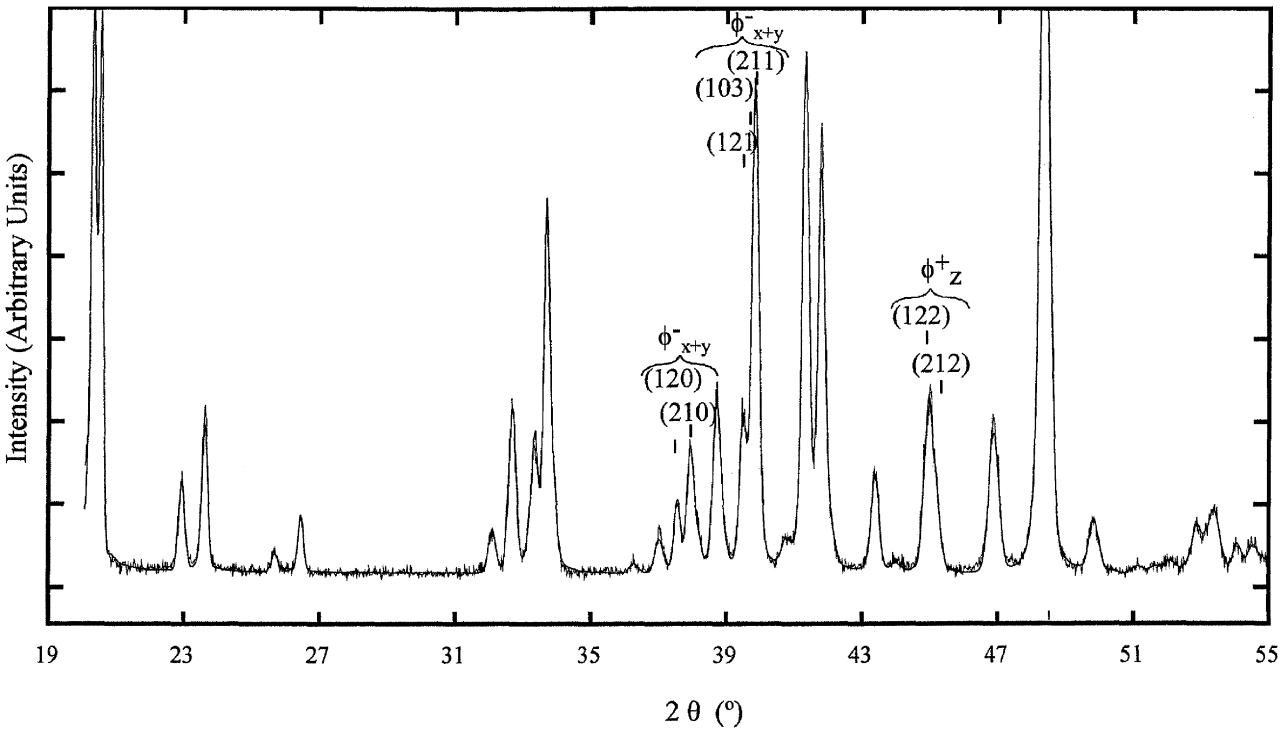

Fig. 2. X-ray diffraction pattern of simmonsite from 19–55° 2θ showing reflections indicative of octahedron tilting (see text).

B-site ordered double perovskite characterized by tilted LiF_6 and AlF_6 octahedra (Fig. 3). Both compounds are examples of the Glazer tilt scheme [15] $a^-b^-c^+$ i.e., two anti-phase and one in-phase rotations of the BF_6 octahedra about three pseudocubic axes. Glazer [16] has shown that when the XRD pattern is indexed in a doubled cubic unit cell ($2a_p \times 2a_p \times 2a_p$) the in-phase and anti-phase rotations will generate superlattice reflections of the type odd–odd–even (*ooe*) and odd–odd–odd (*ooo*). Thus, when transformed to a monoclinic unit cell ($a = \sqrt{2}a_p$; $b = \sqrt{2}a_p$; $c = 2a_p$) doublets such as $\{120, 210\}$ and $\{122, 212\}$ indicate in phase rotation, whereas the triplet $\{121, 103, 211\}$ is indicative of anti-phase rotation of the octahedra. Fig. 2 is an expanded section of the synthetic simmonsite XRD pattern with peaks indicative of the octahedron rotations labelled as φ^-_{x+y} for the two anti-phase rotations and φ^+_z for the in-phase rotation.

Tilting of octahedra in perovskite-type compounds (Fig. 3) is commonly described in terms of a θ-tilt about $[110]_{ap}$, a φ-tilt about $[001]_{ap}$ and a Φ-tilt about $[111]_{ap}$. The Φ-tilt is the resultant of the θ- and φ-tilts [16]. The magnitude of the tilts which reflect the deviation of the structure from that of ideal cubic perovskite can be calculated from the atomic coordinates and lattice parameters using equations given by Groen et al. [17]. These equations have been slightly modified by Mitchell [3] to incorporate the geometrical restriction that when two octahedra of different size are rotated the smaller of the two must always have the greatest rotation angle.

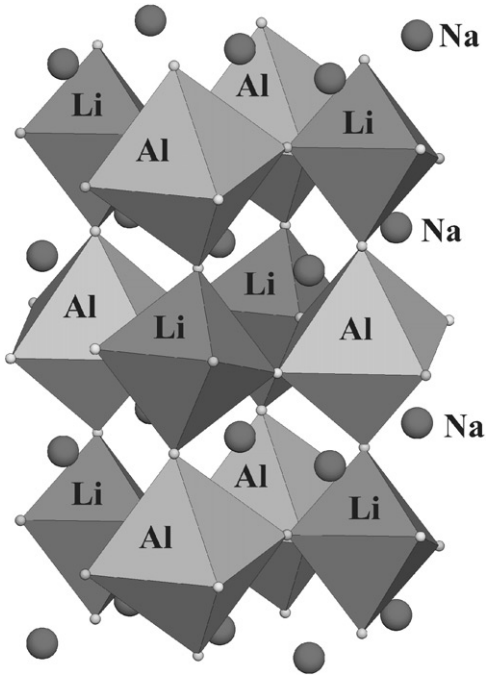

Fig. 3. Polyhedron model of the structure of 1:1 *B*-site ordered Na_2LiAlF_6, showing the tilting and ordering of the LiF_6 and AlF_6 octahedra.

N.B. crystallographic coordinates for synthetic cryolite and simmonsite as presented in Table 3 follow the setting used by Groen et al. [17] for space group $P2_1/n$ (#14), so that their equations for calculating tilt angles

can be used. Table 4 compares the tilt magnitudes and octahedral volumes calculated for synthetic simmonsite and cryolite. Octahedral volumes were calculated using the IVTON coordination analysis software [18]. These data show, as expected, that in simmonsite the smaller AlF_6 polyhedron exhibits greater rotation angles than the larger LiF_6 polyhedron. Rotations are less than found for *B*-site polyhedra in cryolite because this compound has a larger difference in the ionic radii of these cations compared to simmonsite.

Rotations of the octahedra result in the displacement of the fluorine anions away from the *A*-site cation. Significant rotation can cause a reduction in the coordination of the *A*-site cation as fluorine anions are removed from the first coordination sphere. In simmonsite, the Na atoms might be considered as in 10-fold coordination as two of the fluorine atoms are farther from the *A*-site cation than adjacent *B*-site cations. However, bond valence sums (Table 5) suggest that the coordination can also be considered as 8-fold. The greater octahedron rotations displayed by cryolite result in the displacement of a further two fluorine anions for the first coordination sphere leaving the Na cation definitely in 8-fold coordination; a conclusion supported by bond valence sums (Table 5).

Table 5 compares bond lengths and bond valence sums, calculated by the IVTON program [18], for synthetic simmonsite and cryolite together with polyhedron distortion (δ) parameters calculated using equations given by Shannon [19]. Although these parameters are extremely sensitive to the positions of the F anions, these data show that both LiF_6 and AlF_6 octahedra in simmonsite are only very slightly distorted as compared to ideal octahedra ($\delta = 0$) as δ ranges from 0.03 to 0.17. For comparison, $\delta = 0.0017$ for TiO_6 in $CaTiO_3$ and 0.006 for MgF_6 in $NaMgF_3$. The NaF_6 and AlF_6 octahedra in cryolite show less distortion ($\delta_{Al} = 0.013$; $\delta_{Na} = 0.08$) than those occurring in synthetic simmonsite.

In both simmonsite and cryolite *A*-site Na(2) cations are displaced from the centers of the NaF_8 polyhedra by 0.49 and 0.42 Å, respectively (Table 5). For cryolite, this displacement results in significant underbonding of Na(2) and overbonding of Na(1) as indicated by bond valence sums (Table 5). This observation is also valid for structural data given by Hawthorne and Ferguson [14] and Yang et al. [20] for natural and synthetic cryolite, respectively.

In conclusion, we consider that our data indicates that synthetic Na_2LiAlF_6 crystallizes in space group $P2_1/n$ (#14) and is a member of the cryolite structural group. Further, we suggest that these data indicate that the mineral simmonsite also adopts this space group.

Table 4
Octahedron tilt angles and volumes for synthetic simmonsite and cryolite

Simmonsite			Cryolite		
φ	Li	9.3°	φ	Na	10.4°
φ	Al	10.4°	φ	Al	13.0°
θ	Li	11.7°	θ	Na	15.5°
θ	Al	13.5°	θ	Al	19.7°
Φ	Li	14.9°	Φ	Na	18.6°
Φ	Al	17.0°	Φ	Al	23.5°
V_{cell}	213.0 Å^3		V_{cell}	234.8 Å^3	
V_{Li}	11.18 Å^3		V_{Na}	15.15 Å^3	
V_{Al}	8.18 Å^3		V_{Al}	7.99 Å^3	

Table 5
Selected bond lengths (Å) and bond valence for synthetic cryolite and simmonsite

Cryolite		Simmonsite	
A-site cations			
Na(2)	C.N. = 8	C.N. =	8 or 10
F(1)	2.719(4)	F(1)	2.606(6)
F(1)	2.609(4)	F(1)	2.589(5)
F(1)	2.323(4)	F(1)	2.326(6)
F(2)	2.292(5)	F(2)	2.590(5)
F(2)	2.568(5)	F(2)	2.611(6)
F(2)	2.816(5)	F(2)	2.333(5)
F(3)	2.295(6)	F(3)	2.320(4)
F(3)	2.363(6)	F(3)	2.272(4)
		F(3)	3.034(4)
		F(3)	3.059(4)
mean	2.498	*mean*	2.467
δ	6.01	δ	3.07
BV_8	0.985	BV_8	1.014
		BV_{10}	1.064
A-shift	0.415		0.495
B-site cations (1/2,0,0)			
Al–F(1)	1.820(4) × 2	Al–F(1)	1.829(3) × 2
Al–F(2)	1.830(4) × 2	Al–F(2)	1.836(3) × 2
Al–F(3)	1.799(5) × 2	Al–F(3)	1.783(6) × 2
mean	1.816	*mean*	1.816
δ	0.051	δ	0.167
BV_6	2.88	BV_6	2.89
B′-site cations (1/2,0,1/2)			
Na(1)–F(1)	2.211(4) × 2	Li–F(1)	2.037(2) × 2
Na(1)–F(2)	2.271(4) × 2	Li–F(2)	2.036(2) × 2
Na(1)–F(3)	2.273(5) × 2	Li–F(3)	2.062(6) × 2
mean	2.252	*mean*	2.045
δ	0.163	δ	0.034
BV_6	1.27	BV_6	0.94

δ = polyhedral distortion parameter; BV = bond valence sum calculated by IVTON (Balić-Zunić & Vicković [18]).

Acknowledgments

This work was supported by the Natural Sciences and Research Council of Canada and Lakehead University. Alan MacKenzie for assistance with the X-ray diffraction. Two anonymous reviewers of the initial draft this paper are thanked for their positive critical comments.

References

[1] R.H. Mitchell, Rare Earth Minerals Chemistry and Ore Deposits, in: A.P. Jones, F. Wall, C.T. Williams (Eds.), Chapman & Hall, London, 1996, pp. 41–76.
[2] E.E. Foord, J.T. O'Connor, J.M. Hughes, S.J. Sutley, A.U. Falster, A.E. Soregaroli, F.E. Lichte, D.E. Kile, Am. Mineral. 84 (1999) 769–772.
[3] R.H. Mitchell, Perovskites: Modern and Ancient. Almaz Press, Thunder Bay, Ontario, Canada, 2002, 332pp (http://www.almazpress.com).
[4] V. Luana, A. Costales, A. Martin-Pandas, A. Florez, V.H. Garcia-Fernandez, Solid State Commun. 104 (1997) 47–50.
[5] G. Garton, B.M. Wanklyn, J. Am. Ceram. Soc. 50 (1967) 395–399.
[6] J.L. Holm, B.J. Holm, Acta Scand. 24 (1970) 2535–2545.
[7] S.V. Náray-Szabó, Naturwissenschaften 31 (1943) 202–203.
[8] H.T. Stokes, Isotropy Subgroups of the 230 Crystallographic Space Groups, Worldwide Scientific, Singapore, 1988.
[9] M.T. Anderson, K.B. Greenwood, G.A. Taylor, K.R. Poeppelmeier, Prog. Solid State Chem. 22 (1993) 197–233.
[10] P.M. Woodward, Acta Crystallogr. B 53 (1997) 32–43.
[11] M.T. Anderson, K.R. Poepplemeier, Chem. Mater. 3 (1991) 476–482.
[12] J. Laugier, B. Bochu, CELREF. http://www.inpg.fr/LMPG.
[13] J.J. Rodriguez-Carvajal, FULLPROF 2000. Laboratoire Léon Brillouin Saclay, France (http://www.llb.cea.fr/fullweb/powder.htm).
[14] F.C. Hawthorne, R.B. Ferguson, Can. Mineral. 13 (1975) 377–382.
[15] A.M. Glazer, Acta Crystallogr. B 28 (1972) 3384–3392.
[16] A.M. Glazer, Acta Crystallogr. A 31 (1975) 756–762.
[17] W.A. Groen, F.P.F. Van Berkel, D.J.W. Ijdo, Acta Crystallogr. C 42 (1986) 1472–1475.
[18] T. Balić-Zunić, I.J. Vicković, J. Appl. Crystallogr. 29 (1996) 305–306.
[19] R.D. Shannon, Acta Crystallogr. A 32 (1976) 751–767.
[20] H. Yang, S. Ghose, D. Hatch, Phys. Chem. Minerals 19 (1993) 528–544.